# The Effect of Radical Size and Mass on the Cage Recombination Efficiency of Photochemically Generated Radical Cage Pairs

**Jonathan L. Male, Britt E. Lindfors, Katharine J. Covert, and David R. Tyler***

*Contribution from the Department of Chemistry, University of Oregon, Eugene, Oregon 97403*

*Received March 17, 1998*

**Abstract:** This study explored the effect of radical size, chain length, and mass on the radical cage effect. Radical cage pairs of the type [(RCp)(CO)$_3$M$^\bullet$, $^\bullet$M(CO)$_3$(CpR)] (M = Mo or W; CpR = various substituted cyclopentadienyl ligands) were generated by photolysis ($\lambda$ = 540 nm) of the metal−metal bonds in (RCp)$_2$M$_2$(CO)$_6$. The cage recombination efficiencies (denoted as $F_{cP}$) for the radical cage pairs were obtained by extracting them from quantum yield measurements for the photoreactions with $CCl_4$ (a metal-radical trap) as a function of solvent system viscosity. For the series of molecules (R$_3$SiOCH$_2$CH$_2$Cp)$_2$Mo$_2$(CO)$_6$ (R = Me, *i*-Pr, *n*-Pr, *n*-Hx), the $F_{cP}$ values were linearly proportional to mass$^{1/2}$/radius$^2$, in agreement with the predictions of Noyes' cage effect theory. It is also demonstrated that the difference in the cage recombination efficiencies between the [(MeCp)(CO)$_3$Mo$^\bullet$, $^\bullet$Mo(CO)$_3$(CpMe)] and [(MeCp)(CO)$_3$W$^\bullet$, $^\bullet$W(CO)$_3$(CpMe)] cage pairs cannot be ascribed to the different masses of the radicals. Rather, the difference is shown to be attributable to differences in the metal−metal bond energies or to differences in the spin−orbit coupling. In another comparison, $F_{cP}$ at any viscosity for [(MeCp)(CO)$_3$Mo$^\bullet$, $^\bullet$Mo(CO)$_3$(CpMe)] was shown to be identical to that of [Cp*(CO)$_3$Mo$^\bullet$, $^\bullet$Mo(CO)$_3$Cp*] (Cp* = $\eta^5$-C$_5$Me$_5$) in tetrahydrofuran (THF)/tetraglyme solution. Rotation of the MeCp ring is fast compared to the time scale of diffusive separation ($k_{dP}$) and radical recombination ($k_{cP}$), and hence the effective volumes of the radicals in the solvent cage are nearly identical, which leads to similar $F_{cP}$ values.

## Introduction

The concept of the "cage effect" was introduced by Franck and Rabinowitch[1] in 1934 to explain why the efficiency of $I_2$ photodissociation was less in solution than in the gas phase. It was proposed that the solvent temporarily encapsulates the reactive I$^\bullet$ atoms in a "solvent cage," causing them to remain as colliding neighbors before they either recombine or diffuse apart. This concept is illustrated for a general homolysis reaction in eq 1:

$$\mathrm{R{-}R} \underset{k_c}{\overset{k_1 \text{ or } h\nu}{\rightleftharpoons}} \underbrace{(\mathrm{R^\bullet}, {}^\bullet\mathrm{R})}_{\text{cage pair}} \underset{k_D}{\overset{k_d}{\rightleftharpoons}} \underbrace{2\,\mathrm{R^\bullet}}_{\text{free radicals}} \rightarrow \text{products} \quad (1)$$

Note that the formation of free radicals is preceded by the radical cage pair. For quantitative discussions, the "cage recombination efficiency" (denoted as $F_c$) is defined as the ratio of the rate constant for cage recombination ($k_c$) to the sum of the rate constants for all competing cage processes. Thus, in the reaction above $F_c = k_c/(k_c + k_d)$.[2]

Cage effects have an enormous impact on chemical reactivity in solution.[4] In particular, they are necessary to explain a host of kinetic observations and fundamental reaction phenomena. For example, cage effects are necessary to explain magnetic isotope[5,6] and chemically induced dynamic nuclear polarization (CIDNP)[7] effects, rate−viscosity correlations,[8] variations in products and yields as a function of medium,[9] and variations in quantum yields as a function of medium.[10] Examples of important reactions where cage effects are necessary to explain the kinetics include the initiation, propagation, and termination steps of radical polymerization reactions;[11] the reactions of coenzyme $B_{12}$ [12] and its model complexes;[13] the reactions of hemes with $O_2$;[14] and various electron-transfer reactions.[15] New observations of cage effects and their impact on reactivity are

(1) (a) Franck, J.; Rabinowitch, E. *Trans. Faraday Soc*. **1934**, *30*, 120−131. (b) Rabinowitch, E.; Wood, W. C. *Trans. Faraday Soc*. **1936**, *32*, 138l−1387. (c) Rabinowitch, E. *Trans. Faraday Soc*. **1937**, *33*, 1225−1233.

(2) In addition to recombination and diffusive separation, the chemical reactions of cage pairs can include disproportionation, isomerizations, fragmentations, electron transfer, in-cage trapping, and so forth.[3] For the metal-radical cage pairs in this paper, the only chemical process is $k_c$.

(3) Koenig, T.; Hay, B. P.; Finke, R. G. *Polyhedron* **1988**, *7*, 1499−1516.

(4) (a) Lorand, J. P. *Prog. Inorg. Chem.* **1972**, *17*, 207−325. (b) Rice, S. A. *Comprehensive Chemical Kinetics*; Elsevier: Amsterdam, Netherlands, 1985; Vol. 25.

(5) (a) Turro, N. J.; Krautler, B. *Acc. Chem. Res*. **1980**, *13*, 369−377. (b) Turro, N. J. *Proc. Nat. Acad. Sci*. **1983**, *80*, 609−621.

(6) (a) Lott, W. B.; Chagovetz, A. M.; Grissom, C. B. *J. Am. Chem. Soc*. **1995**, *117*, 12194−12201. (b) Natarajan, E.; Grissom, C. B. *Photochem. Photobiol*. **1996**, *64*, 286−295. (c) Grissom, C. B.; Chagovetz, A. M. *Z. Physik. Chem*. **1993**, *182*, 181−188.

(7) (a) Closs, G. *J. Am. Chem. Soc*. **1969**, *91*, 4552−4554. (b) Kaptein, R.; Oosterhoff, R. *Chem. Phys. Lett*. **1969**, *4*, 195−197. (c) Kaptein, R.; Oosterhoff, R. *Chem. Phys. Lett*. **1969**, *4*, 214−216. (d) *Chemically Induced Magnetic Polarization*; Lepley, A. R., Closs, G. L., Eds.; Wiley: New York, 1973. (e) Bethell, D.; Brinkman, M. R. *Adv. Phys. Org. Chem*. **1973**, *10*, 53−128. (f) Kaptein, R. *Adv. Free Radical Chem*. **1975**, *5*, 319−380.

(8) (a) Rembaum, A.; Szwarc, M. *J. Chem. Phys*. **1955**, *23*, 909−913. (b) Pryor, W. A.; Smith, K. *J. Am. Chem. Soc*. **1970**, *92*, 5403−5412. (c) Tanner, D. D.; Meintzer, C. P.; Tsai, E. C.; Oumar-Mahamat, H. *J. Am. Chem. Soc*. **1990**, *112*, 7369−7372.

(9) (a) Tanner, D. D.; Oumar-Mahamat, H.; Meintzer, C. P.; Tsai, E. C.; Lu, T. T.; Yang, D. *J. Am. Chem. Soc*. **1991**, *113*, 5397−5402. (b) Kiefer, H.; Traylor, T. *J. Am. Chem. Soc*. **1967**, *89*, 6667−6671. (c) Koenig, T.; Deinzer, M.; Hoobler, J. A. *J. Am. Chem. Soc*. **1971**, *93*, 938−944. (d) Koenig, T.; Deinzer, M. *J. Am. Chem. Soc*. **1968**, *90*, 7014−7019.

(10) (a) Noyes, R. M. *Z. Elektrochem*. **1960**, *64*, 153−156. (b) Strong, R. L. *J. Am. Chem. Soc*. **1965**, *87*, 3563−3567. (c) Kodama, S. *Bull. Chem. Soc. Jpn*. **1962**, *35*, 658−662. (d) Kodama, S.; Fujita, S.; Takeishi, J.; Toyama, O. *Bull. Chem. Soc. Jpn*. **1966**, *39*, 1009−1014. (e) Hutton, R. F.; Steel, C. *J. Am. Chem. Soc*. **1964**, *86*, 745−746. (f) Abram, I.; Milne, G.; Solomon, B.; Steel, C. *J. Am. Chem. Soc*. **1969**, *91*, 1220−1222. (g) Schaafsma, Y.; Bickel, A.; Kooyman, E. C. *Tetrahedron* **1960**, *10*, 76−80.

10.1021/ja980911x CCC: $15.00 
Published on Web 12/03/1998

reported regularly. For example, analogues of solvent-phase cage effects have now been observed in reactions taking place on surfaces[16] and in gas-phase clusters.[17] In addition, the repercussions of cage effects in supercritical fluids,[18] micelles,[19] zeolites,[20] polymer degradation reactions,[21] and bond cleavage energetics[3,22,23] are areas of intense study.

Despite the recognition that cage effects are important, there is practically no predictive knowledge of the cage effect because virtually nothing systematic or quantitative is known about how changes in radical parameters such as size, shape, mass, and so forth affect the cage effect.[21,24−26] This dearth of information might seem bewildering, given the importance of cage effects, but it is not easy to obtain information about cage effects because it is usually "hidden" from ordinary kinetic observations. In prior papers, however, we reported a new method for obtaining cage effect information in photochemical systems.[27,28] Armed with this new method, we began a research program to investigate the effect of various radical structural parameters on the cage effect. In this initial study, derivatized $Cp_2Mo_2(CO)_6$ molecules were used as the precursors to radical cage pairs. These molecules were chosen because irradiation cleaves the Mo−Mo bond to form $CpMo(CO)_3$ radicals[29] and because the Cp rings can be derivatized, thus allowing changes in the size and mass of the radicals.[30] Reported herein are the results of our investigation on the effect of radical size and mass. One final introductory point follows: $F_c$ for a photochemically formed cage pair does not necessarily equal $F_c$ for the same cage pair formed by thermolysis or by diffusional collision of two free radicals.[25,31] To differentiate these cases, the photochemical cage efficiency will be denoted $F_{cP}$ and the associated rate constants as $k_{cP}$ and $k_{dP}$. A preliminary account of a portion of this work has been previously communicated.[32,33]

**Scheme 1**. Reaction Scheme for the Photolysis of a Metal−Metal Bonded Dimer in the Presence of a Radical Trap (M• = a Metal Radical such as $CpMo(CO)_3$)

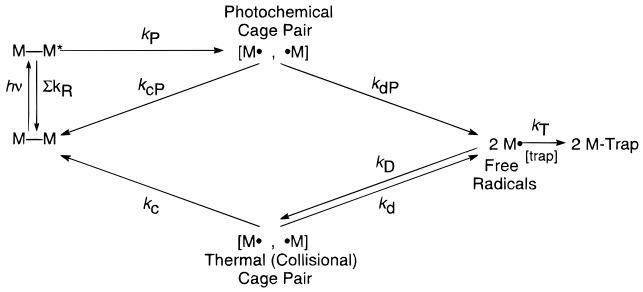


## Results and Discussion

**Method for Measuring $F_{cP}$.** The procedure for obtaining $F_{cP}$ in a photochemical system is based on the measurement of quantum yields for the radical trapping reaction as a function of viscosity. The metal-radical trap used in these studies was $CCl_4$, giving the net reaction in eq 2.[27,29,34,35] This reaction has been extensively studied and the pathway is shown in the top portion of Scheme 1.[29]

$$(RCp)_2Mo_2(CO)_6 \xrightarrow[\text{hexane/mineral oil or THF/tetraglyme}]{h\nu(540\text{ nm}),\ CCl_4} 2\ (RCp)Mo(CO)_3Cl\ [+2\ CCl_3] \quad (2)$$

With sufficiently high concentrations of $CCl_4$, collisional cage pair formation ($k_D$) can be suppressed so that all of the radicals that escape the cage will form the $(RCp)Mo(CO)_3Cl$ product (see below).[27,29c,29d] Under these conditions, the quantum yield for the disappearance of $(RCp)_2Mo_2(CO)_6$ is given by eq 3,

(11) (a) Odian, G. *Principles of Polymerization*, 3rd ed.; Wiley-Interscience: New York, 1991; p 233. (b) Bosch, P.; Mateo, J. L.; Serrano, J. *J. Photochem. Photobiol. A* **1997**, *103*, 177−184. (c) Wolff, E.-H. P.; Bos, A. N. R. *Ind. Eng. Chem. Res*. **1997**, *36*, 1163−1170. (d) Tefera, N.; Weickert, G.; Westerterp, K. R. *J. Appl. Polym. Sci*. **1997**, *63*, 1663−1680.

(12) (a) Garr, C. D.; Finke, R. G. *J. Am. Chem. Soc*. **1992**, *114*, 10440−10445. (b) Finke, R. G. In *Vitamin $B_{12}$ and $B_{12}$ Proteins*, Krautler, B., Ed.; Verlag Chemie: Weinheim, Germany, 1997. (c) Garr, C. D.; Finke, R. G. *Inorg. Chem*. **1993**, *32*, 4414−4421.

(13) (a) Brown, K. L.; Zhou, L. *Inorg. Chem*. **1996**, *35*, 5032−5039. (b) Brown, K. L.; Evans, D. R.; Cheng, S.; Jacobsen, D. W. *Inorg. Chem*. **1996**, *35*, 217−222. (c) Gerards, L. E. H.; Bulthuis, H.; de Bolster, M. W. G.; Balt, S. *Inorg. Chim. Acta* **1991**, *190*, 47−53.

(14) Grogan, T. G.; Bag, N.; Traylor, T. G.; Magde, D. *J. Phys. Chem*. **1994**, *98*, 13791−13796.

(15) (a) van Dijk, H. K.; van der Haar, J.; Stufkens, D. J.; Oskam, A. *Inorg. Chem*. **1989**, *28*, 75−81. (b) Knoll, H.; de Lange, W. J. G.; Hennig, H.; Stufkens, D. J.; Oskam, A. *J. Organomet. Chem*. **1992**, *430*, 123−132. (c) Balzani, V.; Scandola, F. In *Energy Resources Through Photochemistry and Catalysis*, Grätzel, M., Ed.; Academic Press: New York, 1983; p 1. (d) Clark, C. D.; Hoffman, M. Z. *Coord. Chem. Rev*. **1997**, *159*, 359−373.

(16) Jenks, C. J.; Paul, A.; Smoliar, L. A.; Bent, B. E. *J. Phys. Chem*. **1994**, *98*, 572−578.

(17) (a) Vorsa, V.; Nandi, S.; Campagnola, P. J.; Larsson, M.; Lineberger, W. C. *J. Chem. Phys*. **1997**, *106*, 1402−1410. (b) Wang, J.-K.; Liu, Q.; Zewail, A. H. *J. Phys. Chem*. **1995**, *99*, 11309−11320.

(18) (a) Tanko, J. M.; Suleman, N. K.; Fletcher, B. *J. Am. Chem. Soc*. **1996**, *118*, 11958−11959. (b) Bhattacharyya, S.; Bagchi, B. *J. Chem. Phys*. **1997**, *106*, 7262−7267. (c) Materny, A.; Lienau, C.; Zewail, A. H. *J. Phys. Chem*. **1996**, *100*, 18650−18665.

(19) (a) Gould, I. R.; Zimmt, M. B.; Turro, N. J.; Baretz, B. H.; Lehr, G. F. *J. Am. Chem. Soc*. **1985**, *107*, 4607−4612. (b) Tarasov, V. F.; Ghatlia, N. D.; Buchachenko, A. L.; Turro, N. J. *J. Am. Chem. Soc*. **1992**, *114*, 9517−9528. (c) Turro, N. J.; Wu, C.-H. *J. Am. Chem. Soc*. **1995**, *117*, 11031−11032.

(20) Cozens, F. L.; Garcia, H.; Scaiano, J. C. *J. Am. Chem. Soc*. **1993**, *115*, 11134−11140.

(21) (a) Guillet, J. *Polymer Photophysics and Photochemistry*; Cambridge University Press: Cambridge, 1985; p 274. (b) Guillet, J. *Adv. Photochem*. **1988**, *14*, 91−133.

(22) Koenig, T.; Scott, T.; Franz, J. A. Marks, T., Ed.; ACS Symp. Ser. 428; American Chemical Society: Washington, DC, 1990; Chapter 8, pp 113−132.

(23) Koenig, T.; Finke, R. G. *J. Am. Chem. Soc*. **1988**, *110*, 2657−2658.

(24) Loginov, A. V.; Yakovlev, V. A.; Shagisultanova, G. A. *Koord. Khim*. **1989**, *15*, 942−948.

(25) Koenig, T.; Fischer, H. In *Free Radicals*; Kochi, J., Ed.; John Wiley: New York, 1973; Vol. 1, Chapter 4.

(26) Sheldon, R. A.; Kochi, J. K. *J. Am. Chem. Soc*. **1970**, *92*, 4395−4404.

(27) Covert, K. J.; Askew, E. F.; Grunkemeier, J.; Koenig, T.; Tyler, D. R. *J. Am. Chem. Soc*. **1992**, *114*, 10446−10448.

(28) Lindfors, B. E.; Nieckarz, G. F. Tyler, D. R.; Glenn, A. G. *J. Photochem. Photobiol. A: Chem*. **1996**, *94*, 101−105.

(29) (a) Wrighton, M. S.; Ginley, D. S. *J. Am. Chem. Soc*. **1975**, *97*, 4246−4251. (b) Geoffroy, G. L.; Wrighton, M. S. *Organometallic Photochemistry*; Academic Press: New York, 1979. (c) Meyer, T. J.; Caspar, J. V. *Chem. Rev*. **1985**, *85*, 187−218. (d) Laine, R. M.; Ford, P. C. *Inorg. Chem*. **1977**, *16*, 388−391.

(30) (a) Tenhaeff, S. C.; Tyler, D. R. *Organometallics* **1991**, *10*, 473−482. (b) Chen, S.-S.; Wang, J.-X.; Wang, S.-K.; Wang, H.-G. *Jiegou Huaxue* **1993**, *12*, 229−232. (c) Song, L.; Shen, J. *Gaodeng Xuexiao Huaxue Xuebao* **1992**, *13*, 1227−1230.

(31) Koenig, T. In *Organic Free Radicals*; Pryor, W. A., Ed.; ACS Symposium Series 69; American Chemical Society: Washington, DC; 1978; Chapter 9.

(32) Lindfors, B. E.; Male, J. L.; Covert, K. J.; Tyler, D. R. *Chem. Commun*. **1997**, 1687−1688.

(33) Male, J. L.; Lindfors, B. E.; Covert, K. J.; Tyler, D. R. *Macromolecules* **1997**, *30*, 6404−6406.

(34) Scott, S. L.; Espenson, J. H.; Zhu, Z. *J. Am. Chem. Soc*. **1993**, *115*, 1789−1797.

(35) Note that the $^{\bullet}CCl_3$ radicals produced in these reactions do not react further with the metal dimer complexes.[36] In some systems, the $CCl_3$ forms $C_2Cl_6$, but $C_2Cl_4$ is formed in other systems; in no case has $^{\bullet}CCl_3$ been shown to react with a dimer. Thus, the quantum yields are true measures of the photochemical reaction efficiencies.

(36) Tenhaeff, S. C.; Covert, K. J.; Castellani, M. P.; Grunkemeier, J.; Kunz, C.; Weakley, T. J. R.; Koenig, T.; Tyler, D. R. *Organometallics* **1993**, *12*, 5000−5004.

where $\phi_{pair}$ is the quantum yield for formation of the cage pair [$\phi_{pair} = k_P/(k_P + \Sigma k_R)$] and $(1 - F_{cP})$ is the fraction of radical pairs that escape the cage (and which are then trapped by $CCl_4$).

$$\Phi_{obsd} = \phi_{pair}[k_{dP}/(k_{cP} + k_{dP})] = \phi_{pair}[1 - F_{cP}] \qquad (3)$$

Rearranging eq 3 yields eq 4, from which it is clear that $k_{cP}/k_{dP}$ (and in turn $F_{cP}$) can be calculated if $\phi_{pair}$ and $\Phi_{obsd}$ are known.[3,25,27,28] Because $\Phi_{obsd}$ can be measured, the problem of determining $F_{cP}$ thus becomes one of determining $\phi_{pair}$.

$$1/\Phi_{obsd} = [1/\phi_{pair}][1 + k_{cP}/k_{dP}] \qquad (4)$$

Equation 4 was used to obtain $\phi_{pair}$ (and subsequently $F_{cP}$) by measuring the quantum yields for the disappearance of the dimer ($\lambda = 540$ nm) in eq 2 as a function of solvent viscosity. (In this study, a mixture of hexane, mineral oil, and $CCl_4$ (2 M) was used as one of the solvent systems; tetrahydrofuran (THF), tetraglyme, and $CCl_4$ (2 M) was used as another. The viscosity was varied by changing the fraction of viscogen (mineral oil or tetraglyme) in the mixture.[37,38]) If $\phi_{pair}$ and $k_{cP}$ are assumed to be independent of viscosity for a particular solvent system, then the *y*-intercept in a plot of $1/\Phi_{obsd}$ vs viscosity is equal to $1/\phi_{pair}$.[27,28] (For a typical $1/\Phi_{obsd}$ vs viscosity plot see Figure S1 in the Supporting Information.) This statement is shown by eq 4: the second term on the right-hand side contains a viscosity dependence (from the Stokes−Einstein equation: $k_{dP} \propto D \propto 1/\eta$) such that $k_{cP}/k_{dP}$ becomes much smaller than one as the viscosity approaches zero. Thus at zero viscosity $1/\Phi_{obsd}$ will equal $1/\phi_{pair}$.[40,41] A more explicit relationship of $k_{dP}$ to viscosity can also be used: $k_{dP} = (\eta^\circ k_{dP}^\circ/\eta) = k_{dP}/\eta_{rel}$, where $\eta_{rel} = \eta/\eta^\circ$ and the superscript $^\circ$ indicates the value of the parameter at a reference viscosity (taken as the solution without viscogen present in this study).[13a] Equations 5 and 6 are thus obtained.

$$1/\Phi_{obsd} = [1/\phi_{pair}][1 + (k_{cP}/k_{dP}^\circ)\eta_{rel}] \qquad (5)$$

$$F_{cP} = [1 + (k_{dP}/k_{cP})]^{-1} = [1 + (k_{dP}^\circ/k_{cP})(1/\eta_{rel})]^{-1} \qquad (6)$$

A (linear) plot of $1/\Phi_{obsd}$ vs $\eta_{rel}$ then yields an intercept of $1/\phi_{pair}$ and a slope of $(1/\phi_{pair})(k_{cP}/k_{dP}^\circ)$ which then leads to values for $F_{cP}$ via eq 6.

The keys to using this method for obtaining cage effects are an accurate and precise method for measuring quantum yields and a "noncorrelating" method of error analysis. A computerized quantum yield apparatus fulfills the first requirement,[28] and as described in the next section, the bootstrap method of error analysis[42] provides the latter.

**Bootstrapping.** The commonly used $\delta$ method approximation (either differential error analysis or Taylor series expansions) can be used in the determination of confidence limits when the variables are independent and there is no "correlation" between the variables.[43−45] However, in the calculation of $F_{cP}$ (eqs 3−6), the parameters are correlated because $\Phi_{obsd}$ is used to obtain $\phi_{pair}$ and $k_{cP}/k_{dP}$.[27,28] In such instances, the $\delta$ method can still be used, but the procedure is more complicated because it is necessary to obtain and use covariances in the calculations.[43−45] The covariances are not readily calculable, and thus it was necessary to use another method to obtain the confidence limits.

The statistical technique of bootstrapping is a nonparametric procedure to estimate confidence intervals that are not directly obtainable by other methods.[42,46−48] It involves random resampling with replacement of data sets. In this particular case, the sets of $1/\Phi_{obsd}$ (the *y*-term) and viscosity (the *x*-term) pairs (typically 15−21 data point pairs) were used to estimate the confidence limits in $\phi_{pair}$ and $k_{cP}/k_{dP}$. In more specific terms, the assumption of a linear relationship between $1/\Phi_{obsd}$ and relative viscosity was maintained and the 15−21 data pairs[49] were sampled with replacement to generate a plot to which a linear regression was applied and the slope and intercept of the graph were stored in an array; this cycle was repeated 1000 times for each sample.[52] The resulting arrays were used to obtain confidence limits in $1/\phi_{pair}$, $\phi_{pair}$, and $k_{cP}/k_{dP}$. Assuming the error in viscosity to be negligible (i.e., the "within" variance is small compared to the "between" variance;[53] a typical error in viscosity was ≤1%) the confidence limits in $F_{cP}$ were calculated using eq 7.[44,45,54]

$$\mathrm{var}(F_{cP}) = \{\eta_{rel}/[(k_{cP}/k_{dP}^\circ \times \eta_{rel}) + 1]^2\}^2 \times \mathrm{var}(k_{cP}/k_{dP}^\circ) \qquad (7)$$

**Saturation in $CCl_4$.** The method described above for obtaining $F_{cP}$ requires that all free radicals be trapped (i.e., that

(37) The hexane/mineral oil and THF/tetraglyme solvent systems were chosen such that the composition and polarities of solvent and viscogen pairs were extremely similar (see Table 1). This reduces the chance of selective solvation, a condition that could complicate the interpretations of the cage effect.

(38) It is important not to use polymeric viscogens because they can drastically alter the macroviscosity of a solution yet leave the microenvironment unchanged (i.e., they do not change the solvation of the solute). This comes about because large regions of the solvent are still unoccupied by the polymer. As an example of this phenomenon, Szwarc[39] showed that $F_{cP}$ in the photolysis of $CF_3-N{=}N-CF_3$ in $CHCl_3$ did not change when 0.44% poly(ethylene) oxide was added to the solution, yet the macroviscosity increased about 6-fold. In a similar example, Grissom[6c] altered the bulk viscosity of water using Ficoll-400, a polymer of sucrose and epichlorohydrin, yet the viscosity surrounding the solute was relatively unchanged.

(39) Szwarc, M.; Wasserman, B. 160th National Meeting of the American Chemical Society, Chicago, IL, September 1970; American Chemical Society: Washington, DC, 1970; Abstr. POLY 83.

(40) Previous work in supercritical fluids suggests that at low viscosities the yields of products are linear with respect to 1/viscosity and are also an extension of the same plots observed at room temperatures and pressures (see ref 18a).

(41) Whether the extinction coefficients are kept as they are or all averaged has very little effect on the $F_{cP}$ values. The differences do, however, have a small discernible effect on $\Phi_{obsd}$ and hence on the $\phi_{pair}$ values.

(42) Efron, B.; Tibshirani, R. J. *An Introduction to the Bootstrap*; Chapman and Hall: New York, 1993.

(43) Cameron, J. M. In *Encyclopaedia of Statistical Science*; Kotz, S., Johnson, N. L., Read, C. B., Eds.; Wiley-Interscience: New York, 1983; Vol. 2, p 545−551.

(44) Dunn, G. *Design and Analysis of Reliability Studies: the Statistical Evaluation of Measurement Errors*; Oxford University: New York, 1989.

(45) Casella, G.; Berger, R. L. *Statistical Inference*; Brooks/Cole: Pacific Grove, CA, 1990.

(46) Mooney, C. Z.; Duval, R. D. *Bootstrapping: A Nonparametric Approach to Statistical Inference*; Sage University Papers Series on Quantitative Applications in the Social Sciences, Series 07−095, Newbury Park, CA, 1993.

(47) Efron, B. *The JackKnife, the Bootstrap and Other Resampling Plans*; National Science Foundation-Conference Board of the Mathematical Sciences Monograph 38, Philadelphia: Society for Industrial and Applied Mathematics, 1982.

(48) Efron, B.; Tibshirani, R. *Science* **1991**, *253*, 390−395.

(49) Note that within the field of statistics there is some discussion on what is the minimum size of the bootstrap sample that can still yield optimum results.[46−48,50,51]

(50) Schenker, N. *J. Am. Stat. Assoc.* **1985**, *80*, 360−361.

(51) Bickel, P. J.; Krieger, A. M. *J. Am. Stat. Assoc.* **1989**, *84*, 95−100.

(52) The number of iterations of the bootstrap can be shown to yield values that converge quite quickly as the number of iterations reaches 1000 cycles.[42,46]

(53) (a) High, R. R. (Statistics consultant at the University of Oregon Computing Center.) Manuscript in preparation. (b) Myers, R. H. *Classical and Modern Regression with Applications*, 2nd ed.; P. W. S. Publishers: Boston, 1990.

(54) Using eqs 5 and 6 and assuming the error in the value of the viscosity for a particular solution is negligible, we can treat the viscosity as a constant:[44,45,53] $\mathrm{var}(F_{cP}) = [\mathrm{d}(F_{cP})/\mathrm{d}(k_{cP}/k_{dP}^\circ)]^2 \times \mathrm{var}(k_{cP}/k_{dP}^\circ)$; $\mathrm{d}(F_{cP})/\mathrm{d}(k_{cP}/k_{dP}^\circ) = \eta_{rel}/[(\eta_{rel}k_{cP}/k_{dP}^\circ) + 1]^2$.

**Table 1.** Physical Data for the Solvents and Related Molecules Used in This Study

| solvent | relative permittivity (dielectric constant)[a] | molar transition energy, $E_T(30)$ kcal mol$^{-1}$ [b] | thermal conductivity, W m$^{-1}$ K$^{-1}$ [d] | density, g mL$^{-1}$ [e] | absolute viscosity, cP[d] |
|---|---|---|---|---|---|
| $C_4H_8O$ | 7.52 | 37.4 | 0.120 | 0.8892 | 0.456 |
| $C_{10}H_{22}O_5$ | 7.68 | ≈39[c] | 0.1408 | 1.0114 | 4.05[e] |
| $CCl_4$ | 2.2379 | 32.4 | 0.099 | 1.5940 | 0.908 |
| $C_6H_{14}$ | 1.8865 | 31.0 | 0.120 | 0.6603 | 0.300 |
| $C_{12}H_{26}$ | 2.015 | 31.1 | 0.152 | 0.7487 | 1.383 |
| $C_{16}H_{34}$ | 2.0460 | | 0.140 | 0.7733 | 3.032 |
| $C_{18}H_{38}$ | | | 0.150 [f] | 0.7768 [f] | 2.487[g] |
| $C_{22}H_{46}$ | 2.0840 | | | 0.7944 | |

[a] Measured at 20 °C except $C_4H_8O$, which was at 22.0 °C, and $C_{10}H_{22}O_5$ and $C_8H_{18}O_4$, which were at 25.0 °C.[55] [b] At 25 °C and 1 bar.[91] [c] Based on analogous $E_T(30)$ data for diglyme (38.6) and triglyme (38.9).[91] [d] Measured at 25 °C.[55,92] [e] Measured at 20 °C.[55] [f] Measured at 28 °C.[55] [g] Measured at 50 °C.[55]

no radical cage pairs form by diffusion together of free radicals, the $k_D$ step in Scheme 1). This condition was confirmed by studying the quantum yields for the reaction of $Cp_2Mo_2(CO)_6$ with $CCl_4$ in both THF and hexane as a function of [$CCl_4$] (see Figure S2 in the Supporting Information for a plot of $\Phi_{obsd}$ vs [$CCl_4$] in THF). Saturation occurs at about 0.1 M $CCl_4$, indicative of complete free radical trapping. Experiments in this study used [$CCl_4$] = 2 M. Note that a decrease in the quantum yield is observed at ≈10 M (neat $CCl_4$); this downturn is attributed to the increase in viscosity of neat $CCl_4$ (0.908 cP at 25 °C) compared to the THF solutions (0.456 cP at 25 °C) (also see Table 1).[29c,29d,55,56] One final point concerns the possibility of in-cage trapping by the $CCl_4$; a simple calculation shows that no in-cage trapping will occur. The rate constant for the reaction of $CpMo(CO)_3$ with $CCl_4$ is about $10^4$ M$^{-1}$ s$^{-1}$,[29,34,58] whereas that for cage recombination ($k_c$) is ≥$10^9$ s$^{-1}$ and that for diffusional separation ($k_d$) is ≈$10^9$−$10^{10}$ s$^{-1}$.[29c,34,58a] Thus, the reaction of $CCl_4$ with caged $CpMo(CO)_3$ radicals cannot compete with recombination or diffusive separation of the caged pair.[59]

**Synthesis.** The derivatized $Cp_2Mo_2(CO)_6$ molecules **1**−**1** to **4**−**4** used in this study were synthesized by the route shown in eq 8.[32,33,61] (The unconventional numerical nomenclature assigned to these dimers is used to facilitate discussion of their cage pairs. Thus, the cage pair for dimer **1**−**1** becomes [**1**•,•**1**], etc.) The molecules were made rigorously pure by repeated filtrations and recrystallizations from hexanes.

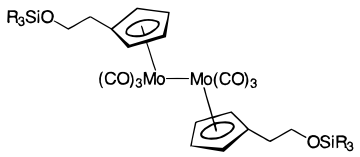


**1-1**, R = Me; **2-2**, R = *i*-Pr; **3-3**, R = *n*-Pr; **4-4**, R = *n*-Hx;
**5-5** has MeCp ligands; **7-7** has Cp* ligands

The −$CH_2CH_2$−spacer was specifically incorporated into these molecules to isolate the Mo−Mo chromophore from any electronic changes caused by varying the R groups.[62] In fact, this strategy worked because the electronic spectra of the four molecules and $(MeCp)_2Mo_2(CO)_6$ (**5**−**5**) are nearly identical.[63] (Each molecule has an intense band at 393 nm in hexane ($\epsilon$ ≈ 20000 cm$^{-1}$ M$^{-1}$), assigned to the $\sigma \rightarrow \sigma^*$ transition, and a weaker band at ≈ 512 nm ($\epsilon$ ≈ 2000 cm$^{-1}$ M$^{-1}$), assigned to a d$\pi \rightarrow \sigma^*$ transition.[29] The irradiations in this study were done at 540 nm; extinction coefficients at this wavelength are reported in Table 2.) This point is important because it suggests that changes in the photophysical parameters will be caused only by differences in the lengths of the side chains and not by electronic differences in the metal−metal bond chromophores.

$$(HOCH_2CH_2Cp)_2Mo_2(CO)_6 \xrightarrow[-80\ °C,\ THF]{n\text{-BuLi}} \text{“}(LiOCH_2CH_2Cp)_2Mo_2(CO)_6\text{”}$$

$$\xrightarrow[-80\ °C,\ THF]{R_3SiCl} (R_3SiOCH_2CH_2Cp)_2Mo_2(CO)_6 \qquad (8)$$

**Size Effects.** The cage effects in molecules **1**−**1** to **4**−**4** were measured and compared in order to probe the effect of radical size on the cage effect. The quantum yields as a function of viscosity in hexane/mineral oil are shown in Figure 1 for the four dimers. Note that at any given viscosity the quantum yields generally decreased in the order **1**−**1** > **2**−**2** > **3**−**3** > **4**−**4**, i.e., the quantum yields decreased as the chain length increased. (Likewise, the $\phi_{pair}$ values follow this trend; see Table 2.) This trend is consistent with our prior observation that the quantum yields for degradation of derivatized metal−metal bonded molecules generally decrease as the chain lengths of the molecules increase.[64] Note, however, that [**5**•,•**5**] does not follow this trend, a result attributable to its relatively low $\phi_{pair}$ value (Table 2). The lower than expected $\phi_{pair}$ value is likely caused by subtle differences in the excited state(s) owing to electronic differences between the −Me group and the −$CH_2CH_2$R groups.[29,65] $F_{cP}$ values for molecules **1**−**1** to **4**−**4** are shown in Figure 2 as a function of viscosity.

(55) *CRC Handbook of Chemistry and Physics*, 76th ed.; Lide, D. R., Ed.; CRC Press: Boca Raton, 1995.

(56) A similar effect has been observed before but not discussed with $Cp_2W_2(CO)_6$ in THF using $CCl_4$ as the radical trap.[29c,29d] The effect of changing the viscosity with the concentration of the radical trap would also explain the trend observed with $Cp_2Mo_2(CO)_6$ in THF with $CHBr_3$ as the radical trap ([$CHBr_3$] = 4.4 × $10^{-2}$ M, $\Phi_D$ = 0.67; [$CHBr_3$] = 8.8 × $10^{-2}$ M, $\Phi_D$ = 0.57; $CHBr_3$ viscosity = 1.89 cP at 25 °C[55]).[57]

(57) Hughey, J. L., IV, Ph.D. Dissertation, University of North Carolina, Chapel Hill, NC, 1975.

(58) (a) Song, J.-S.; Bullock, R. M.; Creutz, C. *J. Am. Chem. Soc*. **1991**, *113*, 9862−9864. (b) Creutz, C.; Song, J.-S.; Bullock, R. M. *Pure Appl. Chem*. **1995**, *67*, 47−54.

(59) Finke recently observed in-cage trapping of ado radicals from the homolysis of adocobalamin.[12a] 2,2,6,6-Tetramethylpiperidinyl-1-oxy (TEMPO) was used as the trap, which has a rate constant for reaction with radicals of $k = 10^7$ M$^{-1}$ s$^{-1}$.[60] The 3 orders of magnitude difference in the rate constant plus the fact that $k_d$ and $k_c$ may be considerably smaller for the large [ado•, •Co(II)binamide] cage pair make in-cage trapping feasible in this system.

(60) Beckwith, A. L. J.; Bowry, V. W.; Ingold, K. U. *J. Am. Chem. Soc*. **1992**, *114*, 4983−4992.

(61) Covert, K. J.; Male, J. L.; Tyler, D. R.; Weakley, T. J. R. *Acta Crystallogr., Sect. C*. Accepted for publication.

(62) The −$CH_2CH_2$− spacer can be viewed as an electronic insulator that reduces any electronic variations on substitution of the alkyl groups. For a similar use of this strategy, see Hughes, R. P.; Trujillo, H. A. *Organometallics* **1996**, *15*, 286−294.

(63) See ref 29 for further discussion of the electronic structures of these metal−metal bonded molecules.

(64) Tenhaeff, S. C.; Tyler, D. R. *Organometallics* **1991**, *10*, 1116−1123.

**Table 2.** Selected Spectroscopic and Photochemical Data

| | in hexane | | | in THF | | |
|---|---|---|---|---|---|---|
| compound | $\epsilon^a$ | $\phi_{pair}$ | $k_c/k_d°$ | $\epsilon^a$ | $\phi_{pair}$ | $k_c/k_d°$ |
| **1**−**1** | 1580 ± 20 | 0.61 ± 0.02 | 0.123 ± 0.012 | 1470 ± 20 | 0.77 ± 0.05 | 0.232 ± 0.051 |
| **2**−**2** | 1530 ± 40 | 0.56 ± 0.02 | 0.139 ± 0.012 | | | |
| **3**−**3** | 1600 ± 60 | 0.55 ± 0.02 | 0.145 ± 0.016 | | | |
| **4**−**4** | 1210 ± 40 | 0.46 ± 0.02 | 0.164 ± 0.018 | 1190 ± 20 | 0.83 ± 0.04 | 0.426 ± 0.045 |
| **5**−**5** | 1670 ± 30 | 0.51 ± 0.01 | 0.112 ± 0.010 | 1530 ± 30 | 0.70 ± 0.03 | 0.214 ± 0.025 |
| **6**−**6**[b] | 1010 ± 100 | 0.58 ± 0.09 | 0.395 ± 0.111 | | | |
| **7**−**7**[c] | | | | 2250 ± 50 | 0.71 ± 0.05 | 0.216 ± 0.060 |

[a] Extinction coefficient at 540 nm in $M^{-1}$ $cm^{-1}$. [b] $(MeCp)_2W_2(CO)_6$. [c] $Cp^*{}_2Mo_2(CO)_6$.

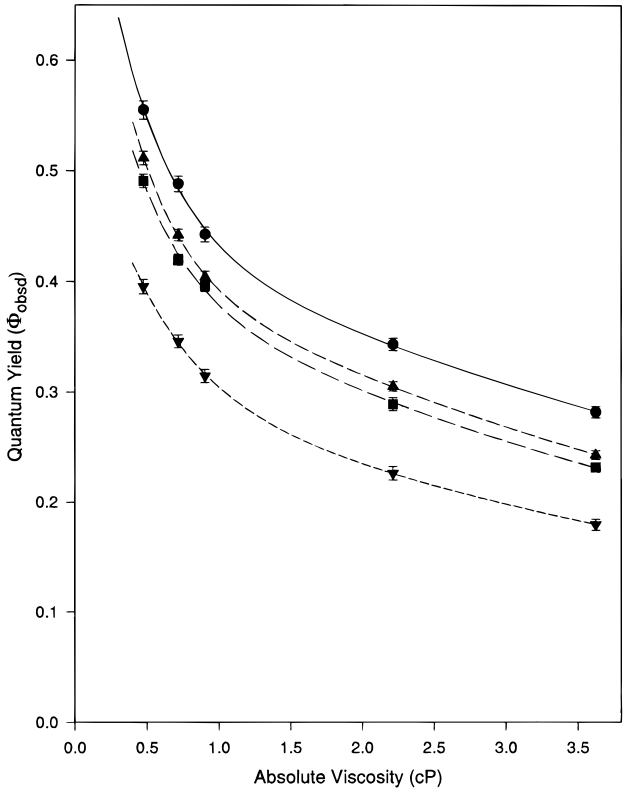


**Figure 1.** Plot of $\Phi_{obsd}$ vs viscosity for the photochemical reaction ($\lambda$ = 540 nm) of $(R_3SiOCH_2CH_2Cp)_2Mo_2(CO)_6$ [R = Me (●), *i*-Pr (▲), *n*-Pr (■), *n*-Hx (▼)] with $CCl_4$ (2 M) at 23 ± 1 °C in hexane/mineral oil. All error bars represent ±1 $\sigma$.

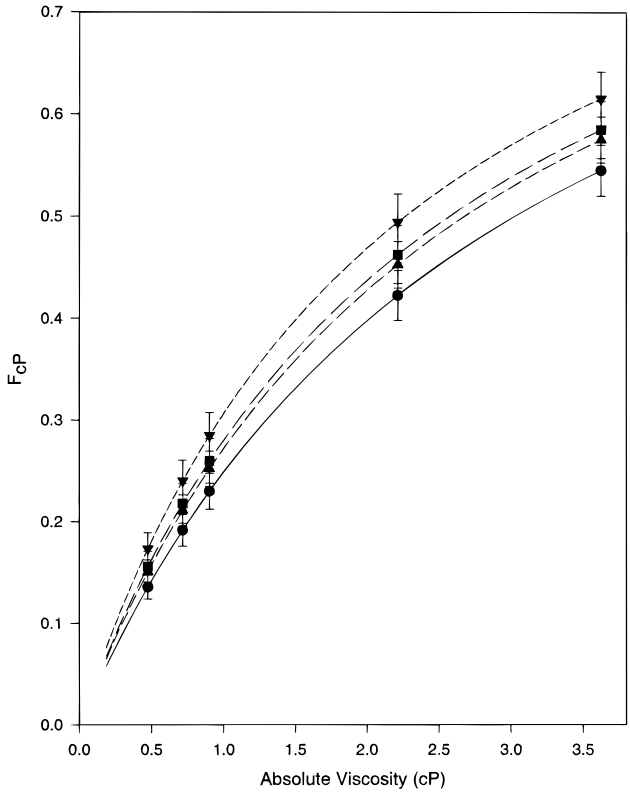


**Figure 2.** Plot of $F_{cP}$ vs viscosity for $(R_3SiOCH_2CH_2Cp)_2Mo_2(CO)_6$ [R = Me (●), *i*-Pr (▲), *n*-Pr (■), *n*-Hx (▼)] with $CCl_4$ (2 M) at 23 ± 1 °C in hexane/mineral oil. All error bars represent ±1 $\sigma$.

Three trends in Figure 2 and Table 2 are important. First, the cage effect increases with increasing length of the substituent on the Cp ligand ([**1**•,•**1**] < [**2**•,•**2**] ≤ [**3**•,•**3**] < [**4**•,•**4**]). Second, $\phi_{pair}$ decreases as the chain length increases. Third, the difference in the cage effects for the four compounds increases as the viscosity increases. (This latter point is required by the Stokes−Einstein equation.[66]) The first conclusion to draw from these results is that both the decrease in $\phi_{pair}$ and the increase in the cage effect ($F_{cP}$) contribute to the smaller quantum yields as the chain lengths increase. However, by using eq 3 and examing the relative changes in $\phi_{pair}$ and $F_{cP}$ we show that the differences in $\phi_{pair}$ are largely responsible for the differences in $\Phi_{obs}$ at any particular viscosity. Thus, even at the highest viscosities, where the differences in the cage effects between the molecules are most pronounced, only about one-third of the difference in $\Phi_{obsd}$ between [**1**•,•**1**] and [**4**•,•**4**] is due to the difference in $F_{cP}$ between the two molecules (see Table 2 and the Supporting Information in Table S1 for relevant data for compounds **1**−**1** to **4**−**4**). The bulk of the difference is due to the differences in $\phi_{pair}$ between the two molecules.

To quantify the size effects in Figure 2, the results were compared to Noyes' cage effect model.[10a,67] In his mathematical description of the cage effect, Noyes predicted that the cage effect will increase as radical size increases and as radical mass decreases.[67] Specifically, he predicted that the ratio $k_{dP}/k_{cP}$ (which is equal to $(F_{cP}{}^{-1}-1)$) is proportional to $m^{1/2}/r^2$, where r is the radius of the radical and *m* is the mass.[25,68] Plots of $(F_{cP}{}^{-1}-1)$ vs $m^{1/2}/r^2$ for molecules **1**−**1** to **5**−**5** are shown in Figure 3. (Each line in the figure shows data for a different viscosity.) Note the excellent fit of the experimental results to the prediction for molecules **1**−**1** to **4**−**4**. Also note that the

(65) (a) Abel, E. W.; Singh, A.; Wilkinson, G. *J. Chem. Soc.* **1960**, 1321−1324. (b) Wilkinson, G.; U. S. Patent 3,109,010, 1963; *Chem. Abstr.* **1964**, *60*, 14538d.

(66) The modified Stokes−Einstein equation (for slip conditions) is $D = kT/4\eta\pi r$, where *D* is the diffusion coefficient of the radical, $\eta$ is the viscosity, and *r* is the hydrodynamic radius of the spherical radical. As the viscosity increases, all other terms are constant for a particular molecule, and the diffusion coefficient, which relates to $k_d$ or $k_{dP}$, will lead to a divergence of the $F_c$ or $F_{cP}$ values for the series of molecules at higher viscosities.

(67) (a) Noyes, R. M. *J. Chem. Phys.* **1954**, *22*, 1349−1359. (b) Noyes, R. M. *Prog. React. Kinet.* **1961**, *1*, 129−160. (c) Noyes, R. M. *J. Am. Chem. Soc.* **1955**, *77*, 2042−2045. (d) Noyes, R. M. *J. Am. Chem. Soc.* **1956**, *78*, 5486−5490.

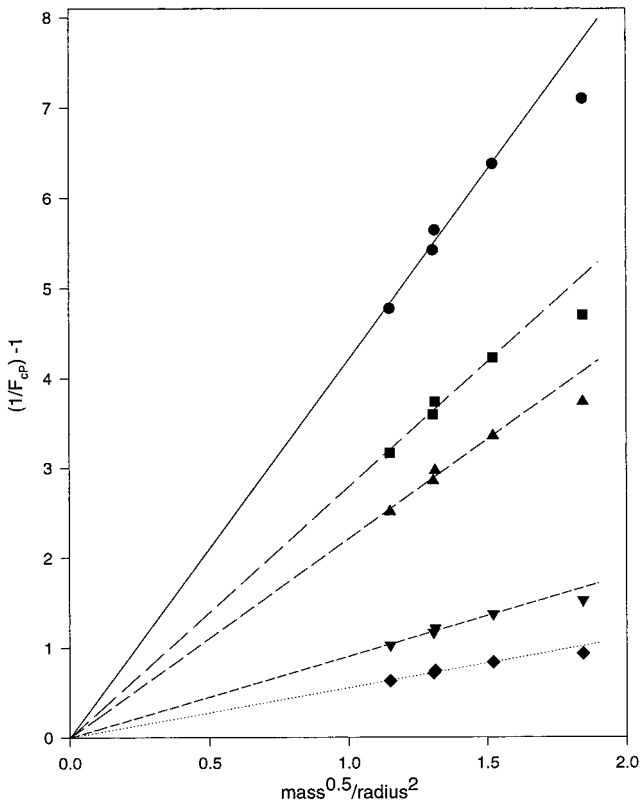


**Figure 3.** Plot of $F_{cP}^{-1}-1$ vs $m^{1/2}/r^2$ ($m$ = mass of the radical; $r$ = the radius of a sphere with the same volume as the static volume of the radical) for $(R_3SiOCH_2CH_2Cp)_2Mo_2(CO)_6$ (R = Me, *i*-Pr, *n*-Pr, *n*-Hx) and $(MeCp)_2Mo_2(CO)_6$ (in this order left to right) at the measured viscosities of: 0.47 (●), 0.72 (■), 0.90 (▲), 2.2 (▼), 3.6 (◆) cP.

best-fit lines all intercept at the origin as required by Noyes' equation in footnote 68. One major conclusion of this paper is that, for a similar series of radical cage pairs, the cage effects for these pairs vary with radius$^{-2}$ and with mass$^{1/2}$. (The radii used in Figure 3 are "effective radii." They were obtained by calculating the radii of spheres with volumes equivalent to those of the radicals. The procedure for determining the volumes of the radicals is described in the Experimental Section.)

Note that the values of $k_{dP}/k_{cP}$ for molecule **5**−**5** are somewhat lower than predicted by the lines in Figure 3. This result may be caused by two effects. First, radical **5**• has a different shape than **1**•−**4**•; models show that **5**• is approximately spherical, while the shapes of **1**•−**4**• are elongated. (See Figure S3 for a comparison of molecular shapes.) It is suggested that the data points for **5**• are not on the lines because the relationship between the (static) radical volume and the "effective radius" for radicals **1**•−**4**• is not followed exactly for radical **5**•; **5**• has a fundamentally different shape. Second, the MeCp ring is rotating rapidly (whereas the $CpCH_2CH_2OSiR_3$ rings are probably not). As shown below, in THF solution the cage effect behavior of **5**• is essentially identical to that of the Cp*Mo(CO)$_3$ radical, a result that is attributed to rapid MeCp ring rotation in **5**•. Ring rotation will increase the effective "swept-out volume" of **5**• and, in turn, the effective radius, which would move the points for **5**• to the left and hence closer to the line.

By increasing the chain length, both the size and mass of the radicals are increased (Table 3). The quantum yield and $F_{cP}$ results in Figures 1 and 2 are consistent with the effects from increased volume predominating over those of increased mass (if an increase in chain length is taken as representing an increase in size). (This finding also agrees with the relationship of $k_{dP}/k_{cP}$ to $m^{1/2}/r^2$ for which there is a greater dependence on radius than mass.[68]) In fact, as Table 3 shows, the proportional increase in mass is not nearly as large as the proportional increase in size. Also note that the competing factors of size and mass might be responsible for the relatively small influence of $F_{cP}$ compared to $\phi_{pair}$ in their effect on $\Phi_{obsd}$. In other words, the increase in mass somewhat counteracts the influence of the increase in volume on the cage effect as the chain length increases.[69]

The question remains: why does $\phi_{pair}$ decrease as the chain length increases? This could be a manifestation of the well-known phenomenon in which radiationless decay is faster in molecules with more vibrational modes.[70]

**Results in THF.** To check on the generality of the results described above, the experiments were repeated in THF solution for [**1**•,•**1**], [**4**•,•**4**], and [**5**•,•**5**]. In these experiments, tetraglyme ($CH_3(OCH_2CH_2)_4OCH_3$) was used as the viscogen. Quantum yield data are shown in Figure 4 and cage effect results are in Figure 5. In brief, the same trends found in hexane solution were also found in THF, i.e., the cage effect increases as the length of the side chain on the Cp ring increases; likewise, the quantum yield for disappearance of **4**−**4** is smaller than that of **1**−**1**.

**Comparison of THF to Hexane.** Although the same trends were found in THF as in hexane, there are quantitative differences in the two solvents. In each case, the cage effect at a particular viscosity is larger in THF than in hexane.[71] (Figures S4, S5, and S6 in the Supporting Information show plots of $F_{cP}$ vs viscosity for the [**1**•,•**1**], [**4**•,•**4**], and [**5**•,•**5**] radical cage pairs in both hexane/mineral oil and THF/tetraglyme.) Several features of the solvent systems could account for this result: preferential solvation may be occurring;[37] THF may be coordinating to the radicals in the cage to form a 19-electron complex that prevents recombination of the cage pair; the "thermal cage effect" may be operating;[72] there may be differences in the conformational preferences of the solute molecules in the two solvent systems; and finally, the masses and densities of the solvent molecules may be important in determining the magnitude of the cage effect. Space does not permit a discussion of these factors in this paper, but a more complete discussion is found in the Supporting Information and will be probed thoroughly in a future publication.[73]

**The Effect of Radical Mass on $F_{cP}$.** In a prior study, we showed that the cage effect for the photogenerated [**5**•,•**5**] radical pair was smaller than that for the similarly sized but more massive W analogue, [(MeCp)(CO)$_3$W•, •W(CO)$_3$(CpMe)]

(68) From the Noyes model:[25] $k_d/k_c = [(R_0 - 2b)/2b] + (R_0/2b)\{[(A_T + \alpha A_E)/\alpha](^1/\eta) + [(A_T\alpha A_E)/\alpha](^1/\eta)^2\}$, where: $A_T = [(^3/_2)mkT]^{1/2}/(6\pi b^2)$; $A_E = [m(h\nu - E)]^{1/2}/(6\pi b^2)$; $R_0$ is the initial separation of the radicals; $b$ is the diffusion radius of the radical, $\alpha$ is the probability of reaction per collision; $\eta$ is the solvent viscosity; $m$ is the mass of the radical; $\nu$ is the frequency of the absorbed photon; and $E$ is the dissociation energy of the process. In our series of Mo−Mo dimers, at a single wavelength, temperature and viscosity, the sole variables are $m$, $b$, and $\alpha$. If it can be assumed that the third term [containing $(^1/\eta)^2$] is negligible compared to the second term [containing $(^1/\eta)$], then $k_d/k_c$ might vary as a function of $m^{1/2}/b^2$, if the probability of reaction per collision of the series of radicals is similar. Indeed, it might be speculated that the deviation of **5**−**5** from the trend for **1**−**1** to **4**−**4** might be a consequence of a variation in $\alpha$.

(69) Studies to separate the mass and volume effects on $F_{cP}$ are currently being investigated in our laboratory.

(70) Ferraudi, G. J. *Elements of Inorganic Photochemistry*; Wiley-Interscience: New York, 1988; p 101.

(71) Also note that the $\phi_{pair}$ values for a particular molecule are larger in THF/tetraglyme than in hexane/mineral oil (see Table 2). The increase in $\phi_{pair}$ may be a consequence of the solvent polarity.

(72) Langford, C. H.; Shaw, L. E. *Coord. Chem. Rev.* **1997**, *159*, 221−233.

(73) Braden, D. A.; Parrack, E.; Male, J. L.; Tyler, D. R. Unpublished results.

**Table 3.** Mass and Volume Data for the Radicals and Solvents

| monomeric solute or solvent molecule | molecular mass, g mol$^{-1}$ | static molecular volume,[a,b] Å$^3$ | approximate longest molecular axis, Å | approximate maximum dynamic spherical volume,[a,b] Å$^3$ |
|---|---|---|---|---|
| **1**$^\bullet$ | 361.3 | 185 | 12.23 | 958 |
| **2**$^\bullet$ | 445.4 | 270 | 13.37 | 1250 |
| **3**$^\bullet$ | 445.4 | 272 | 14.68 | 1660 |
| **4**$^\bullet$ | 571.7 | 397 | 18.38 | 3250 |
| **5**$^\bullet$ | 259.1 | 108 | 6.95 | 176 |
| **6**$^\bullet$ | 347.0 | 108 | 6.95 | 176 |
| **7**$^\bullet$ | 315.2 | 162 | 7.02 | 181 |
| $C_6H_{14}$ | 86.2 | 97 | 10.49 | 604 |
| $C_{20}H_{42}$ | 282.6 | 298 | 28.05 | |
| $C_4H_8O$ | 72.1 | 59 | 6.47 | 142 |
| $CH_3(OCH_2CH_2)_4OCH_3$ | 222.3 | 161 | 18.98 | |
| $CCl_4$ | 153.8 | 89 | 6.45 | 141 |

[a] The volumes in some instances are slightly different from those reported in ref 33 because of further energy minimizations of the geometries. [b] The static volume can be viewed as a minimum value[88] and the dynamic isotropic rotation value can be viewed as a maximum volume value.

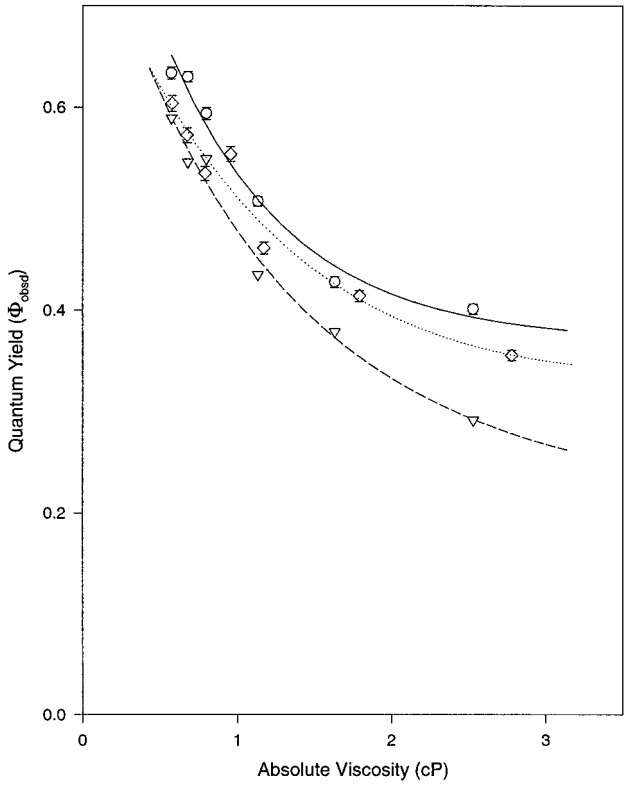


**Figure 4.** Plot of $\Phi_{obsd}$ vs viscosity for the photochemical reaction ($\lambda$ = 540 nm) of $(CpMe)_2Mo_2(CO)_6$ (◇), $(Me_3SiOCH_2CH_2Cp)_2Mo_2(CO)_6$ (○), $[(n\text{-}Hx)_3SiOCH_2CH_2Cp)]_2Mo_2(CO)_6$ (▽) with $CCl_4$ (2 M) at 23 ± 1 °C in THF/tetraglyme. All error bars represent ±1 $\sigma$.

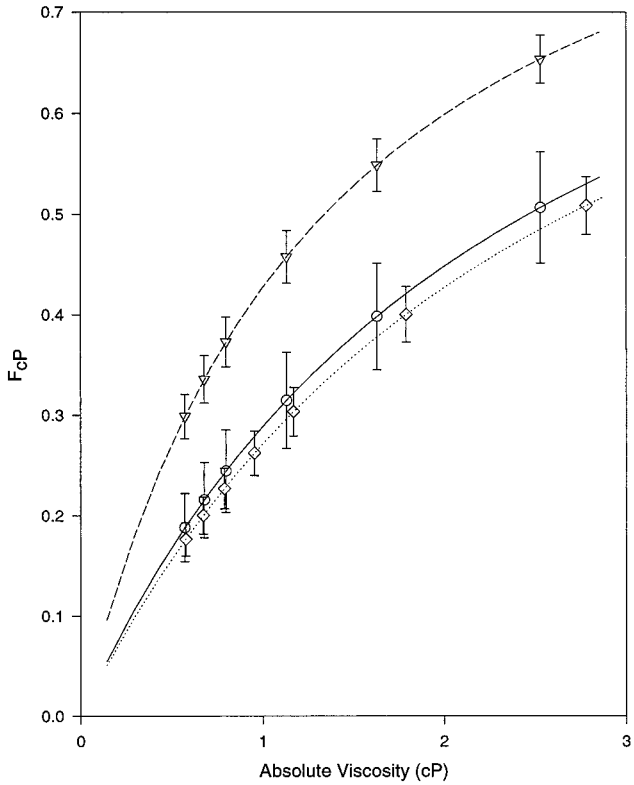


**Figure 5.** Plot of $F_{cP}$ vs viscosity for the photochemical reaction ($\lambda$ = 540 nm) of $(MeCp)_2Mo_2(CO)_6$ (◇), $(Me_3SiOCH_2CH_2Cp)_2Mo_2(CO)_6$ (○), $[(n\text{-}Hx)_3SiOCH_2CH_2Cp)]_2Mo_2(CO)_6$ (▽) with $CCl_4$ (2 M) at 23 ± 1 °C in THF/tetraglyme. All error bars represent ±1 $\sigma$.

([**6**$^\bullet$,$^\bullet$**6**]).[27] It was hypothesized that the difference in mass was responsible for the differences in the cage effects, although several other factors, e.g., M−M bond energies and spin−orbit coupling, might also account for the differences. To probe the effect of mass on the cage effect, $F_{cP}$ for the [**1**$^\bullet$,$^\bullet$**1**] cage pair was compared to $F_{cP}$ values for [**5**$^\bullet$,$^\bullet$**5**] and [**6**$^\bullet$,$^\bullet$**6**]. The [**1**$^\bullet$,$^\bullet$**1**] cage pair was investigated because radical **1**$^\bullet$ has about the same mass (361.3 g/mol) as the **6**$^\bullet$ radical (347.0 g/mol). Thus, a comparison of $F_{cP}$ values for [**1**$^\bullet$,$^\bullet$**1**] to [**5**$^\bullet$,$^\bullet$**5**] (259.1 g/mol for the **5**$^\bullet$ radical, also see Table 3) shows the effect of a heavier radical mass on $F_{cP}$, while at the same time the metal−metal bond and the spin−orbit coupling parameters are identical.

$F_{cP}$ values for photochemically generated [**1**$^\bullet$,$^\bullet$**1**], [**5**$^\bullet$,$^\bullet$**5**], and [**6**$^\bullet$,$^\bullet$**6**] cage pairs were obtained in the usual way by measuring the quantum yields for reaction with $CCl_4$ as a function of viscosity (see Supporting Information, Figure S7). Plots of the cage effect ($F_{cP}$) vs viscosity for the three dimers are shown in Figure 6. Note that at any viscosity, the cage effects increase in the order [**5**$^\bullet$,$^\bullet$**5**] ≈ [**1**$^\bullet$,$^\bullet$**1**] ≪ [**6**$^\bullet$,$^\bullet$**6**]. The large difference in $F_{cP}$ between the [**6**$^\bullet$,$^\bullet$**6**] and [**1**$^\bullet$,$^\bullet$**1**] cage pairs (which have about the same mass) and the similarity in the cage effects for the [**1**$^\bullet$,$^\bullet$**1**] and [**5**$^\bullet$,$^\bullet$**5**] cage pairs show that the difference in the radical masses is not responsible for the difference in $F_{cP}$ reported earlier between [**5**$^\bullet$,$^\bullet$**5**] and [**6**$^\bullet$,$^\bullet$**6**].

The difference in the cage effects for the [**5**$^\bullet$,$^\bullet$**5**] (or [**1**$^\bullet$,$^\bullet$**1**]) and [**6**$^\bullet$,$^\bullet$**6**] cage pairs may be attributed to several factors. One possible factor is the smaller difference between the bond dissociation energy and the photochemical excitation energy for $(MeCp)_2W_2(CO)_6$ compared to $(RCp)_2Mo_2(CO)_6$ (R = Me or $-CH_2CH_2OSiMe_3$).[74] The excess photonic energy for Mo may lead to an increase in translational energy in the photogenerated

(74) $D_{W-W} \approx 56$ kcal mol$^{-1}$; $D_{Mo-Mo} \approx 32$ kcal mol$^{-1}$; [75] $h\nu = 52$ kcal mol$^{-1}$.

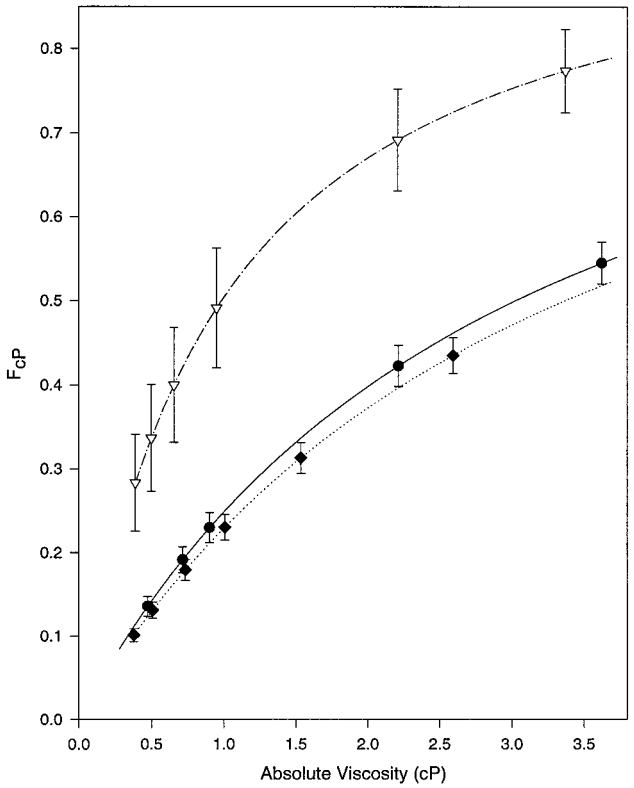


**Figure 6.** Plot of $F_{cP}$ vs viscosity for the $(Me_3SiOCH_2CH_2Cp)_2Mo_2(CO)_6$ (●), $(MeCp)_2Mo_2(CO)_6$ (◆), $(MeCp)_2W_2(CO)_6$ (▽) molecules with $CCl_4$ (2 M) in hexane/mineral oil at 23 ± 1 °C. All error bars represent ±1 $\sigma$.

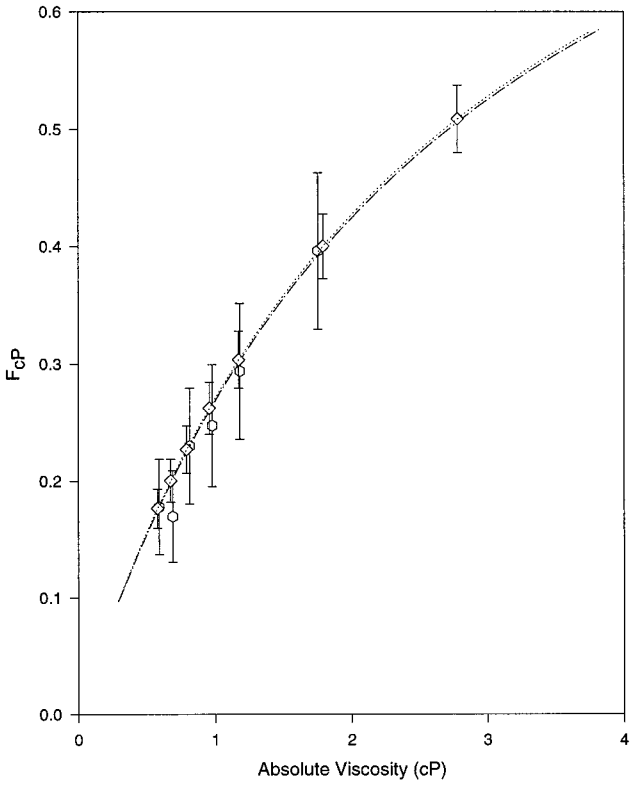


**Figure 7.** Plot of $F_{cP}$ vs viscosity for the photochemical reaction ($\lambda$ = 540 nm) of $(MeCp)_2Mo_2(CO)_6$ (◇), and $Cp^*_2Mo_2(CO)_6$ (⬡) molecules with $CCl_4$ (2 M) in THF/tetraglyme at 23 ± 1 °C. All error bars represent ±1 $\sigma$.

radicals and a consequent decrease in the cage effect. In the photolysis of $I_2$ in solution, Noyes showed that the quantum yield for homolysis increased as the energy of the exciting radiation increased.[10a,67] He proposed that energy in excess of the bond dissociation energy ended up in the kinetic energy of the atoms, which increased the probability of escape from the cage; i.e., the cage effect decreased. For multiatom radicals, it is unknown if the excess energy is quickly dissipated to vibrational modes or if the fragments will retain some of their excess energy in the form of translational energy.[25] Alternatively, the larger cage effect for the [**6**$^\bullet$,$^\bullet$**6**] cage pair may reflect the increased driving force (and consequently lower activation barrier) for the recombination of the two W radicals compared to the Mo radicals.[76] A third explanation is the increase in spin−orbit coupling for W compared to Mo. Spin−orbit coupling may be a factor because homolysis is thought to occur from a triplet state to yield a triplet radical cage pair.[77] Thus, there may possibly be a spin barrier to recombination. An increase in spin−orbit coupling will facilitate intersystem crossing of the triplet cage pair to the singlet cage pair, and hence the rate of cage pair recombination will be enhanced.[25]

It might be argued that the differences in $F_{cP}$ between the [**1**$^\bullet$,$^\bullet$**1**] and [**6**$^\bullet$,$^\bullet$**6**] cage pairs depicted in Figure 6 are attributable to a size effect.[78] This explanation is unlikely because, as our results above showed, the cage efficiency increases as the radicals get larger, contrary to the trend observed with [**1**$^\bullet$,$^\bullet$**1**] and [**6**$^\bullet$,$^\bullet$**6**].

**MeCp vs Cp*.** Cage effect data for $(MeCp)_2Mo_2(CO)_6$ ([**5**−**5**]) and $Cp^*_2Mo_2(CO)_6$ ([**7**−**7**]) in THF are shown in Figure 7. Note that the cage effects are essentially identical at all viscosities despite the larger static volume of the Cp* ligand (Table 3). These results are intriguing because the conclusions drawn in the preceding sections might lead one to predict that the cage effect in [**7**$^\bullet$,$^\bullet$**7**] should be larger because it is a larger molecule. However, the results with [**5**−**5**] and [**7**−**7**] are explainable if MeCp ring rotation is fast compared to the $k_{cP}$ and $k_{dP}$ processes (generally $k_{rotation} \geq 10^{11}$ s$^{-1}$ [79]). If ring rotation is fast then the effective size (dynamic volume, Table 3) swept out by the rotating MeCp ligand is equal to that of the Cp* ligand and one would not expect differences in the cage effect as a result of static volume.

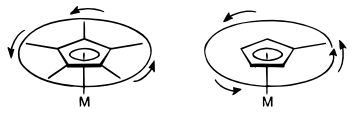


(75) (a) Krause, J. R.; Bininosti, D. R. *Can. J. Chem.* **1975**, *53*, 628−632. (b) Landrum, J. T.; Hoff, C. D. *J. Organomet. Chem.* **1985**, *282*, 215−224. (c) Amer, S.; Kramer, G.; Poë, A. J. *J. Organomet. Chem.* **1981**, *209*, C28−C30.

(76) The reaction coordinate diagrams for the two complexes would look like this. (To facilitate the comparison of the curves, the energies of the two cage pairs are shown as equal.)

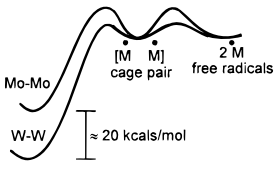


See, Lowry, T. H.; Richardson, K. S. *Mechanism and Theory in Organic Chemistry*, 3rd ed.; Harper and Row: New York, 1987; p 213.

(77) Stiegman, A. E.; Tyler, D. R. *Coord. Chem. Rev.* **1985**, *63*, 217−240.

(78) The static molecular volumes and approximate longest molecular axis of the mononuclear radicals are shown in Table 3.

(79) Aime, S.; Braga, D.; Cordero, L.; Gobetto, R.; Grepioni, F.; Righi, S.; Sostero, S. *Inorg. Chem.* **1992**, *31*, 3054−3059.

**Key Conclusions and Insights.** An important general point to emphasize is that the organometallic radical cage pairs in this study have cage recombination efficiencies in the range 0.1−0.9. This is noteworthy because, as indicated by Finke and Koenig,[3] many quantitative mechanistic conclusions are based on the assumption that $F_c$ is equal to either 1.0 or zero. In fact, $F_{cP}$ (and $F_c$) values span this range, and the proper interpretation of numerous data requires therefore that $F_c$ be known.

This study also showed that, in radical cage pairs of the type $[(R_3SiOCH_2CH_2Cp)(CO)_3Mo^{\bullet}, {}^{\bullet}Mo(CO)_3(CpCH_2CH_2OSiR_3)]$, the ratio $k_d/k_c$ $[(F_{cP}{}^{-1}) - 1]$ is proportional to $m^{1/2}/r^2$, where $r$ is the radius of the radical, assumed to be spherical, and $m$ is the mass. The radicals used in this study are not spherical, but as Figure 3 shows, one way around this problem is to use an "effective radius", which is equal to the radius of a sphere that has a volume equal to the static volume of the radical. The linearity in Figure 3 might be fortuitous, and results with other radical pairs have yet to be collected to test if this is an acceptable way to treat these data. Note that, for a homologous series of radicals, an increase in mass is usually accompanied by an increase in size; the former will decrease $F_{cP}$ and the latter will increase $F_{cP}$. The results herein suggest that the effects from increased volume predominate over those of increased mass in a homologous series.

This nearly equal cage effect for radical cage pairs consisting of the $(MeCp)(CO)_3Mo^{\bullet}$ ($5^{\bullet}$) and $Cp^*(CO)_3Mo^{\bullet}$ ($7^{\bullet}$) radicals was interpreted as indicating that the rapid MeCp ring rotation creates a larger effective volume for $5^{\bullet}$ than is predicted by its static size. Generalization of this result leads to the hypothesis that molecular movements on the time scale of the cage lifetime (or faster) will affect the value of $F_{cP}$ if such movements increase the effective volume of the radical.

A comparison of the $[(MeCp)(CO)_3Mo^{\bullet}, {}^{\bullet}Mo(CO)_3(CpMe)]$ and $[(MeCp)(CO)_3W^{\bullet}, {}^{\bullet}W(CO)_3(CpMe)]$ cage pairs led to the conclusion that when one wishes to examine mass and steric effects on $F_{cP}$, it is necessary to compare systems that have the same radical−radical bond and bond energies. In early studies of the cage effect, this point was less of a concern because a carbon−carbon bond formed in nearly every system studied. Organometallic systems involve a much more varied selection of radical pairs, and it will be important to consider that differences in bond energies, spin−orbit coupling, and so forth may dominate any variations caused by differences in size and mass of the radicals.

## Experimental Section

**Materials and Reagents.** All manipulations were carried out in the absence of water and atmospheric oxygen using standard Schlenk line and drybox techniques. The molecules $(MeCp)_2M_2(CO)_6$ (M = Mo, W) and $(\eta^5\text{-}C_5Me_5)_2Mo_2(CO)_6$ were prepared as described in the literature.[27,80,81] The solvents *n*-hexane (HPLC grade, Aldrich), THF (Aldrich), and tetraglyme (tetraethyleneglycol dimethyl ether, Aldrich) were purified using standard laboratory procedures.[82] Mineral oil (Spectrum) was stirred over sodium and then filtered under nitrogen. The radical trap $CCl_4$ (Fisher) was distilled twice from $P_2O_5$ and passed through a column of basic alumina. All solvents were degassed by repeated freeze−pump−thaw cycles and stored in amber bottles under nitrogen prior to use.

Molybdenum hexacarbonyl (Aldrich) and *n*- and *sec*-butyl-lithium in cyclohexane (Aldrich) were used without further purification. The compound 2-bromoethan-1-ol (Aldrich) was fractionally distilled. Dicyclopentadiene (Aldrich) was cracked into an ice-bath immediately prior to use. Trimethylsilyl chloride, tri-*n*-propylsilyl chloride, tri-*iso*-propylsilyl chloride, and tri-*n*-hexylsilyl chloride were all purchased from Aldrich and were used without purification if $^1$H NMR spectra indicated the absence of impurities. Otherwise, the trialkyl silyl chloride compounds were purified by drying over $CaH_2$ and distilling under $N_2$ (or under reduced pressure in the case of propyl and hexyl substituted derivatives). The $(HOCH_2CH_2Cp)_2Mo_2(CO)_6$ complex was prepared via modifications of procedures previously reported in the literature.[30a,83]

The mixed solvent systems were prepared in a darkened drybox. All solutions were 20% (v/v)(≈2 M) $CCl_4$, with varying ratios of either *n*-hexane and mineral oil (from 0 to 60% mineral oil by volume) or THF and tetraglyme (from 0 to 80% tetraglyme by volume). Kinematic viscosities of the solutions were measured at 23 ± 1 °C with calibrated Cannon−Fenske viscometers. The kinematic viscosities and densities of these solutions were then used to calculate the absolute viscosities.

**Instrumentation and Procedures.** Infrared spectra were recorded on a Nicolet Magna 550 FT-IR spectrometer with OMNIC software. Samples were prepared as either KBr pellets or as solutions in $CaF_2$ cells (path length 0.109 mm). UV−vis spectra were recorded with either a Perkin-Elmer Lambda 6 or a Beckman DU UV−vis spectrophotometer. All UV−vis spectrophotometers were calibrated with holmium oxide and neutral density filters. NMR spectra were collected on a Varian Unity/Inova 300 spectrometer at an operating frequency of 299.95 and 75.43 MHz for $^1$H and $^{13}$C nuclei, respectively. Elemental analyses were performed by E + R Microanalytical Laboratory, Inc., Corona, NY.

Quantum yields ($\lambda$ = 540 nm) were determined utilizing an Oriel Merlin system equipped with an Oriel 200 W high-pressure mercury arc lamp.[28] The silicon photodiode in the Merlin system was calibrated with Aberchrome 540 [84] (i.e., by irradiating at 540 nm and monitoring the drop in absorbance at 494 nm, all at 23 ± 1 °C). Recently, concerns over the use of Aberchrome 540 have arisen for irradiations at ∼366 nm.[84c,85] The calibration was therefore verified with Reinecke's salt.[86] The intensity calculated with Aberchrome 540 was always slightly less (≈ 8%) than that with Reinecke's salt; the appropriate corrections were therefore made.

The bootstrapping technique was executed using the bootstrap library (obtained from the Carnegie-Mellon University statistics archive),[42] S-plus software, and a routine written in S-plus to obtain slope and intercept information for a linear regression. Typically 15−21 data pairs of $1/\Phi_{obsd}$ vs viscosity data were in a sample on which 1000 iterations of the bootstrap were carried out. The subsequently calculated arrays of data were analyzed to yield mean values and variances of $1/\phi_{pair}$, $\phi_{pair}$, slope, and $k_{cP}/k_{dP}°$. Each complete calculation was repeated three times.

The static molecular volumes of the dimeric molecules were calculated using the Steric computer program and the approximate volumes of the radicals were obtained as half the output for the binuclear species.[87] The ($x$, $y$, $z$) coordinates of the molecules were created by geometric optimizations of the molecules in the Spartan program using semiempirical calculations [PM3(TM)] and via Babel converted to a suitable format for Steric. The volume occupied in space by the molecule (not the volume encased by an outer covering surface) was

(80) Birdwhistell, R.; Hackett, P.; Manning, A. R. *J. Organomet. Chem.* **1978**, *157*, 239−241.

(81) (a) Ginley, D. S.; Wrighton, M. S. *J. Am. Chem. Soc.* **1975**, *97*, 3533−3535. (b) Ginley, D. S.; Bock, C. R.; Wrighton, M. S. *Inorg. Chim. Acta* **1977**, *23*, 85−94.

(82) Perrin, D. D.; Armarego, W. L. F. *Purification of Laboratory Chemicals*, 3rd ed.; Pergamon: Oxford, 1988.

(83) (a) Schröder, V. R.; Striegler, A.; Zimmerman, G.; Mühlstädt, M. *J. Prakt. Chem.* **1973**, *315*, 958−964. (b) Tenhaeff, S. C. Ph.D. Thesis, University of Oregon, Eugene, OR, June 1991. (c) Keana, J. F. K.; Ogan, M. D. *J. Am. Chem. Soc.* **1986**, *108*, 7951−7957.

(84) (a) Heller, H. G.; Langan, J. R. *J. Chem. Soc., Perkin Trans. 2* **1981**, 341−343. (b) Heller, H. G.; Langan, J. R. *EPA Newslett.* **1981**, *12*, 71−73. (c) Heller, H. G. *EPA Newslett.* **1993**, *47*, 44.

(85) (a) Guo, Z.; Wang, G.; Tang, Y.; Song, X. *J. Photochem. Photobiol. A.; Chem.* **1995**, *88*, 31−34. (b) Uhlmann, E.; Gauglitz, G. *J. Photochem. Photobiol. A.; Chem.* **1996**, *98*, 45−49.

(86) (a) Adamson, A. W.; Wilkins, R. G. *J. Am. Chem. Soc.* **1954**, *76*, 3379−3385. (b) Adamson, A. W. *J. Am. Chem. Soc.* **1958**, *80*, 3183−3189. (c) Adamson, A. W.; Sporer, A. H. *J. Am. Chem. Soc.* **1958**, *80*, 3865−3870. (d) Wegner, E. E.; Adamson, A. W. *J. Am. Chem. Soc.* **1966**, *88*, 394−404.

(87) The computer program Steric was written by B. Craig Taverner, Department of Chemistry, Witwatersrand, Private Bag 3, WITS 2050, Johannesburg, South Africa.

calculated using the van der Waals radii, then a rectangular box was fitted around the molecule and a Monte Carlo sampling of a minimum of 400,000 points was collected. The number of points found inside the molecule was multiplied by the volume of the box and then divided by the total number of points.[88] The idealized structures in Spartan were utilized to obtain the approximate maximum distance across the dimeric molecule. These in turn were utilized to obtain approximate maximum dynamic volumes of the molecules, if the assumption of rapid isotropic tumbling is valid.

**Synthesis of 1−1.** To a −80 °C (dry ice/acetone) solution of $(HOCH_2CH_2Cp)_2Mo_2(CO)_6$ (0.309 g, 0.524 mM) in THF (25 mL) in a Schlenk tube was added *n*-BuLi (0.72 mL, 1.2 mM) dropwise over 20 min. After 1 h of reaction time, stirring was ceased and the brick red solid was allowed to settle. The clear supernatant was removed via cannula and the solid was washed with multiple cold THF washes until the supernatant was colorless. Fresh THF (25 mL, −80 °C) was added to the precipitate and to the mixture was added $(CH_3)_3SiCl$ (0.0905 mL, 1.05 mM). The reaction was allowed to proceed until the solution turned clear and deep burgundy (∼3 h). The solution was allowed to warm to room temperature and the solvent was removed in vacuo. In a drybox, hexanes (≥10 mL) were added to the solid (in order to dissolve the compound and remove the hexane insoluble impurities), the resultant opaque burgundy mixture was filtered through a glass frit, and the solvent was removed from the filtrate in vacuo. Any residual impurities were removed by eluting a minimum volume hexane solution of the material through a basic alumina column (1 in.). Only the dark burgundy bands were collected and the hexanes removed in vacuo to result in the purified solid. Additional purification was afforded by recrystallization of the compound from hexanes/THF if required. The overall yield was 85%. $^1$H NMR ($C_6D_6$): $\delta$ 0.06 (s, br, 18 H, $CpCH_2CH_2OSi(CH_3)_3$), 2.37 (t, 4 H, $J$ = 6.3 Hz, $CpCH_2CH_2OSi(CH_3)_3$, 3.42 (t, 4 H, $J$ = 6.3 Hz, $CpCH_2CH_2OSi(CH_3)_3$), 4.78 (t, 4 H, $J$ = 2.3 Hz, $CpCH_2CH_2OSi(CH_3)_3$), 4.93 (t, 4 H, $J$ = 2.3 Hz).[89] $^{13}$C{$^1$H} NMR ($C_6D_6$): $\delta$ −0.5 (s, $CpCH_2CH_2OSi(CH_3)_3$), 32.4 (s, $CpCH_2CH_2OSi(CH_3)_3$), 63.5 (s, $CpCH_2CH_2OSi(CH_3)_3$, 91.7 (s, $CpCH_2CH_2OSi(CH_3)_3$), 94.1 (s, $CpCH_2CH_2OSi(CH_3)_3$), 110.4 (s, $CpCH_2CH_2OSi(CH_3)_3$). IR (KBr), $\nu$(CO): 1951 (s), 1907 (s), 1890 (s) cm$^{-1}$; (hexanes), $\nu$(CO): 2016 (vw), 1957 (s), 1917 (s), 1906 (sh) cm$^{-1}$. UV−vis (hexanes) $\lambda_{max}$ ($\epsilon$, M$^{-1}$ cm$^{-1}$): 394 (19 900 ± 900), 513 (2100 ± 20) nm. Anal. Calcd for $C_{26}H_{34}Mo_2O_8Si_2$: C, 43.22; H, 4.74. Found: C, 42.99; H, 4.62.

**Synthesis of 2−2.** The complex was prepared as previously described for **1−1** using $(HOCH_2CH_2Cp)_2Mo_2(CO)_6$ (0.250 g, 0.424 mM), *n*-BuLi (0.58 mL, 0.93 mM), and $(CH_3CH_2CH_2)_3SiCl$ (0.185 mL, 0.848 mM). The overall yield of the burgundy solid **2−2** was 66%. $^1$H NMR ($C_6D_6$): $\delta$ 0.60 (t, 12 H, $J$ = 9.0 Hz, $CpCH_2CH_2OSi(CH_2CH_2CH_3)_3$), 1.02 (t, 18 H, $J$ = 6.9 Hz, $CpCH_2CH_2OSi(CH_2CH_2CH_3)_3$), 1.41 (m, 12 H, $CpCH_2CH_2OSi(CH_2CH_2CH_3)_3$), 2.40 (m, 4 H, $CpCH_2CH_2OSi(CH_2CH_2CH_3)_3$), 3.49 (t, 4 H, $J$ = 6.0 Hz, $CpCH_2CH_2OSi(CH_2CH_2CH_3)_3$), 4.80 (t, 4 H, $J$ = 2.3 Hz, $CpCH_2CH_2OSi(CH_2CH_2CH_3)_3$), 4.97 (t, 4 H, $J$ = 2.3 Hz, $CpCH_2CH_2OSi(CH_2CH_2CH_3)_3$).[89] $^{13}$C{$^1$H} NMR ($C_6D_6$): $\delta$ 16.7 (s, $CpCH_2CH_2OSi(CH_2CH_2CH_3)_3$), 17.2 (s, $CpCH_2CH_2OSi(CH_2CH_2CH_3)_3$), 18.6 (s, $CpCH_2CH_2OSi(CH_2CH_2CH_3)_3$), 32.5 (s, $CpCH_2CH_2OSi(CH_2CH_2CH_3)_3$), 63.9 (s, $CpCH_2CH_2OSi(CH_2CH_2CH_3)_3$), 91.8 (s, $CpCH_2CH_2OSi(CH_2CH_2CH_3)_3$), 93.9 (s, $CpCH_2CH_2OSi(CH_2CH_2CH_3)_3$). IR (KBr), $\nu$(CO): 1956 (vs), 1917 (vs), 1905 (vs) cm$^{-1}$; (hexanes), $\nu$(CO): 2016 (vw), 1957 (s), 1916 (s), 1906 (sh) cm$^{-1}$. UV−vis (hexanes) $\lambda_{max}$ ($\epsilon$, M$^{-1}$ cm$^{-1}$): 393 (19 000 ± 400), 512 (2110 ± 60) nm. Anal. Calcd for $C_{38}H_{58}Mo_2O_8Si_2$: C, 51.23; H, 6.56. Found: C, 51.46; H, 6.82.

**Synthesis of 3−3.** The complex was prepared as previously described for **1−1** using $(HOCH_2CH_2Cp)_2Mo_2(CO)_6$ (0.254 g, 0.430 mM), *n*-BuLi (0.59 mL, 0.95 mM), and $((CH_3)_2CH)_3SiCl$ (0.184 mL, 0.861 mM). The overall yield of the burgundy solid **3−3** was 44%. $^1$H NMR ($C_6D_6$): $\delta$ 1.06 (s, $CpCH_2CH_2OSi(CH(CH_3)_2)_3$), 1.10 (m, $CpCH_2CH_2OSi(CH(CH_3)_2)_3$), 2.39 (t, 4 H, $J$ = 6.2 Hz, $CpCH_2CH_2OSi(CH(CH_3)_2)_3$), 3.55 (t, 4 H, $J$ = 6.0 Hz, $CpCH_2CH_2OSi(CH(CH_3)_2)_3$), 4.79 (t, 4 H, $J$ = 2.1 Hz, $CpCH_2CH_2OSi(CH(CH_3)_2)_3$), 4.99 (t, 4 H, $J$ = 2.4 Hz, $CpCH_2CH_2OSi(CH_2CH_2CH_3)_3$).[89] $^{13}$C{$^1$H} NMR ($C_6D_6$): $\delta$ 12.2 (s, $CpCH_2CH_2OSi(CH(CH_3)_2)_3$), 18.2 (s, $CpCH_2CH_2OSi(CH(CH_3)_2)_3$), 32.7 (s, $CpCH_2CH_2OSi(CH(CH_3)_2)_3$), 64.7 (s, $CpCH_2CH_2OSi(CH(CH_3)_2)_3$), 91.8, 94.0, 110.5 (s, $CpCH_2CH_2OSi(CH(CH_3)_2)_3$). IR (KBr), $\nu$(CO): 1943 (vs), 1912 (s), 1889 (vs) cm$^{-1}$; (hexanes), $\nu$(CO): 2015 (vw), 1957 (s), 1917 (s), 1906 (sh) cm$^{-1}$. UV−vis (hexanes) $\lambda_{max}$ ($\epsilon$, M$^{-1}$ cm$^{-1}$): 393 (20 100 ± 800), 512 (2080 ± 30) nm. Anal. Calcd for $C_{38}H_{58}Mo_2O_8Si_2$: C, 51.23; H, 6.56. Found: C, 51.15; H, 6.73.

**Synthesis of 4−4.** The complex was prepared as previously described for **1−1** using $(HOCH_2CH_2Cp)_2Mo_2(CO)_6$ (0.286 g, 0.484 mM), *n*-BuLi (0.67 mL, 1.1 mM), and $[CH_3(CH_2)_5]_3SiCl$ (0.355 mL, 0.968 mM). The resultant burgundy red oil did not crystallize upon cooling to −40 °C; the overall yield of **4−4** was 84%. $^1$H NMR ($C_6D_6$): $\delta$ 0.77−0.60 (m, $CpCH_2CH_2OSi(CH_2(CH_2)_4CH_3)_3$), 0.95−0.90 (m, $CpCH_2CH_2OSi(CH_2(CH_2)_4CH_3)_3$), 1.45−1.31 (m, $CpCH_2CH_2OSi(CH_2(CH_2)_4CH_3)_3$), 2.46 (t, 4 H, $J$ = 6.2 Hz, $CpCH_2CH_2OSi(CH_2(CH_2)_4CH_3)_3$), 3.57 (t, 4 H, $J$ = 6.0 Hz, $CpCH_2CH_2OSi(CH_2(CH_2)_4CH_3)_3$), 4.84 (t, 4 H, $J$ = 2.1 Hz, $CpCH_2CH_2OSi(CH_2(CH_2)_4CH_3)_3$), 5.01 (t, 4 H, $J$ = 2.4 Hz, $CpCH_2CH_2OSi(CH_2(CH_2)_4CH_3)_3$).[89] $^{13}$C{$^1$H} NMR ($C_6D_6$): $\delta$ 14.4 (s, $CpCH_2CH_2OSi(CH_2(CH_2)_4CH_3)_3$), 15.6 (s, $CpCH_2CH_2OSi(CH_2(CH_2)_4CH_3)_3$), 23.0, 23.6, 32.0 (s, $CpCH_2CH_2OSi(CH_2(CH_2)_4CH_3)_3$), 32.7 (s, $CpCH_2CH_2OSi(CH_2(CH_2)_4CH_3)_3$), 33.8 (s, $CpCH_2CH_2OSi(CH_2(CH_2)_4CH_3)_3$), 64.0 (s, $CpCH_2CH_2OSi(CH_2(CH_2)_4CH_3)_3$), 91.8 (s, $CpCH_2CH_2OSi(CH_2(CH_2)_4CH_3)_3$), 94.0 (s, $CpCH_2CH_2OSi(CH_2(CH_2)_4CH_3)_3$), 110.5 (s, $CpCH_2CH_2OSi(CH_2(CH_2)_4CH_3)_3$). IR (KBr), $\nu$(CO): 1957 (vs), 1914 (vs) cm$^{-1}$; (hexanes), $\nu$(CO): 2015 (vw), 1957 (s), 1916 (s) 1906 (sh) cm$^{-1}$. UV−vis (hexanes) $\lambda_{max}$($\epsilon$, M$^{-1}$ cm$^{-1}$): 393 (16 000 ± 700), 513 (1640 ± 30) nm. Anal. Calcd for $C_{56}H_{94}Mo_2O_8Si_2$: C, 58.83; H, 8.29. Found: C, 58.99; H, 8.48.

**Photochemical Reactions of $[R_3SiOCH_2CH_2Cp]_2Mo_2(CO)_6$ (R = Me, *n*-Pr, *i*-Pr, *n*-Hx) (1−1 to 4−4), $(MeCp)_2M_2(CO)_6$ (M = Mo, W) (5−5, 6−6) and $(C_5Me_5)_2Mo_2(CO)_6$ (7−7).** A stock solution was prepared with 20% (v/v) $CCl_4$ and the appropriate amount of viscogen. (For example, 10% (v/v) mineral oil in *n*-hexane was prepared by pipetting 20.00 mL of $CCl_4$ and 10 mL of mineral oil into a 100.00 mL volumetric flask and diluting with *n*-hexane up to the graduated mark.)[90] Additional *n*-hexane (4−7 mL) was then added to ensure that four 25.00 mL aliquots and a solvent reference could be taken from the same stock solution. The masses of the samples were determined and the complexes transferred via multiple washings with the stock solution to volumetric flasks (25.00 mL) inside a darkened drybox. The concentrations of the samples were selected in order to afford absorbance readings of between 0.8 and 1.5 at 540 nm. Aliquots (4.00 mL) of each compound in the solution of a specific viscosity were pipetted into each of three cuvettes (1 cm path length) equipped with a freeze−pump−thaw bulb (as a sidearm) and a stir bar. Each cuvette was then degassed by four freeze−pump−thaw cycles and allowed to thermally equilibrate for at least 1 h before photolysis in the Merlin apparatus (an Oriel 200 W high-pressure mercury arc lamp coupled with a Beckman DU monochromator and a Merlin radiometer system).

(88) White, D.; Coville, N. J. *Adv. Organomet. Chem.*, **1994**, *36*, 95−158.

(89) In the $^1$H NMR spectra of these complexes, the Cp protons are only apparent triplets. This is probably due to the cyclopentadienyl derivative being an AA′BB′ spin system; the apparent triplet is probably overlapping doublets.

(90) The approximate ratios of solvent/viscogen/$CCl_4$ in the stock solutions and their respective approximate viscosities were

| approximate ratio of solvent/viscogen/$CCl_4$ | approximate viscosity, cP *n*-hexane/mineral oil/$CCl_4$ | approximate viscosity, cP THF/tetraglyme/$CCl_4$ |
|---|---|---|
| 80:0:20 mL | 0.38 | 0.58 |
| 70:10:20 mL | 0.51 | 0.67 |
| 60:20:20 mL | 0.74 | 0.79 |
| 50:30:20 mL | 1.01 | 0.95 |
| 40:40:20 mL | 1.54 | 1.17 |
| 30:50:20 mL | 2.59 | |
| 20:60:20 mL | 5.00 | 1.79 |
| 0:80:20 mL | | 2.78 |

(91) Reichardt, C. *Solvents and Solvent Effects in Organic Chemistry*, 2nd ed.; VCH: Weinheim, 1988; pp. 365−371.

(92) Yaws, C. L. *Handbook of Thermal Conductivity−Library of Physico-Chemical Property Data−Organic Compounds C8 to C28*; Gulf Publishing: Houston, 1995; Volume 3.

Use of the Merlin apparatus has been reported previously.[28] Light intensity ($\lambda = 540$ nm) was determined by actinometry using Aberchrome 540 in toluene ($\phi_{540} = 0.0484$)[84] and Reinecke's salt ($\phi_{545} = 0.282$).[86] Over a period of 20 min, 101 intensity observations were collected, of which those 26 observations between 5 and 10 min were used for the determinations of quantum yields. In determining the $\Phi_{obsd}$, $\phi_{pair}$, and $F_{cP}$ parameters, average molar absorptivity values were used for complexes **1**−**1** to **4**−**4** (for complexes **1**−**1** to **4**−**4**: $1570 \pm 36$ in *n*-hexane; for **1**−**1** and **4**−**4**: $1470 \pm 15$ in THF) because $\lambda_{max}$ values and molar absorptivities at this wavelength for the complexes are similar. The difference between the extinction coefficients of the oil-like complex **4**−**4** and the other molecules is ascribed to minor experimental errors even after repeated measurements.[41]

**Acknowledgment.** Acknowledgment is made to the National Science Foundation for the support of this work. B.E.L. was supported by a fellowship from the National Physical Science Consortium. This paper is dedicated to Professor Richard M. Noyes (1919−1997), who played a pioneering role in our understanding of the cage effect. We thank Audun S. Runde and Robin R. High for their invaluable assistance with programming in S-Plus, the theory of the bootstrap, and statistical advice. Dr. B. C. Taverner is thanked for a copy of Steric and his invaluable assistance with the program. Dale A. Braden is acknowledged for his insightful comments.

**Supporting Information Available:** Three pages of discussion, two pages of additional references, two additional tables, and nine additional figures showing the additional quantum yields and $F_{cP}$ vs viscosity plots for molecules **1**−**1** to **7**−**7** not shown in the text; space-filling pictures of the dimers; a bulk density plot vs $F_{cP}$ plot; a percent viscogen vs viscosity plot; a $1/\Phi_{obsd}$ vs viscosity plot; two tables showing all the quantum yields, and $F_{cP}$ data for **1**−**1** to **6**−**6**; also a discussion comparing THF to hexane (16 pages, print/PDF). See any current masthead page for ordering information and Web access instructions.

JA980911X